LETTER

doi:10.1038/nature10462

Coherent coupling of a superconducting flux qubit to an electron spin ensemble in diamond

Xiaobo Zhu[1], Shiro Saito[1], Alexander Kemp[1], Kosuke Kakuyanagi[1], Shin-ichi Karimoto[1], Hayato Nakano[1], William J. Munro[1], Yasuhiro Tokura[1], Mark S. Everitt[2], Kae Nemoto[2], Makoto Kasu[1], Norikazu Mizuochi[3,4] & Kouichi Semba[1]

During the past decade, research into superconducting quantum bits (qubits) based on Josephson junctions has made rapid progress[1]. Many foundational experiments have been performed[2–8], and superconducting qubits are now considered one of the most promising systems for quantum information processing. However, the experimentally reported coherence times are likely to be insufficient for future large-scale quantum computation. A natural solution to this problem is a dedicated engineered quantum memory based on atomic and molecular systems. The question of whether coherent quantum coupling is possible between such natural systems and a single macroscopic artificial atom has attracted considerable attention[9–12] since the first demonstration of macroscopic quantum coherence in Josephson junction circuits[2]. Here we report evidence of coherent strong coupling between a single macroscopic superconducting artificial atom (a flux qubit) and an ensemble of electron spins in the form of nitrogen–vacancy colour centres in diamond. Furthermore, we have observed coherent exchange of a single quantum of energy between a flux qubit and a macroscopic ensemble consisting of about 3×10^7 such colour centres. This provides a foundation for future quantum memories and hybrid devices coupling microwave and optical systems.

With the early successes of single-atom quantum state manipulation[13], research in quantum information processing with atomic systems has largely progressed independently from that using solid-state systems. In recent years, considerable effort has been devoted to coupling atomic and molecular systems to solid-state qubits to form hybrid quantum devices[9–11]. Hybrid devices involving the integration of an ensemble of atomic spin systems with a transmission line resonator have been realized[14–18]. Such schemes have the potential to couple superconducting solid-state qubits to optical fields via atomic systems, thus allowing quantum media conversion. The coupling strength, g, of an individual atomic system to one electromagnetic mode in a resonator circuit is usually too small for the coherent exchange of quantum information. However, the coupling strength of an ensemble of N such atomic systems will be enhanced by a factor of $\sqrt{N}$ (ref. 19), making it possible to reach the strong-coupling regime ($g\sqrt{N} \gg \kappa$ and $g\sqrt{N} \gg \gamma$, where κ and γ are the respective damping rates of the resonator circuit and the atomic system).

Of the many possible hybrid systems, coupling a flux qubit to a nitrogen–vacancy colour centre (NV^- centre) in diamond is particularly appealing. First, the magnetic coupling strength between a flux qubit and a single NV^- centre can be three orders of magnitude larger than that between a superconducting transmission line resonator and an NV^- centre[12]. Second, the ground state of a NV^- centre is a triplet ($S = 1$) owing to its C_{3v} symmetry (Fig. 1b). The $S = 1$ state $|m_S = 0\rangle$ is separated by 2.88 GHz from the near-degenerate excited states $|m_S = \pm 1\rangle$ under zero magnetic field (Fig. 1c). This energy separation is ideal for a gap-tunable flux qubit to be brought into and out of resonance with it.

In this Letter, we report the observation of vacuum Rabi oscillations between a flux qubit and an ensemble of approximately 3×10^7 NV^- centres in diamond. This demonstrates strong coherent coupling between two dissimilar quantum systems with a collective coupling constant of $g_{ens} \approx 70$ MHz.

We begin by describing our experimental set-up (Fig. 1). A sample of diamond containing NV^- centres was prepared by ion implantation of $^{12}C^{2+}$ at 700 keV under high vacuum into single-crystal, type-1b diamond synthesized under high pressure and at high temperature (HPHT) and with (001) surface orientation. The $^{12}C^{2+}$ ions, implanted with a surface density of 3×10^{13} cm^{-2}, were stopped at a depth of 600^{+50}_{-100} nm. This generated vacancies with a concentration of order 5×10^{18} cm^{-3} over a depth of ~0.7 μm. After implantation, the crystals were annealed at 900 °C under vacuum for 3 h. This high-dose carbon implantation method enhances the yield of generated

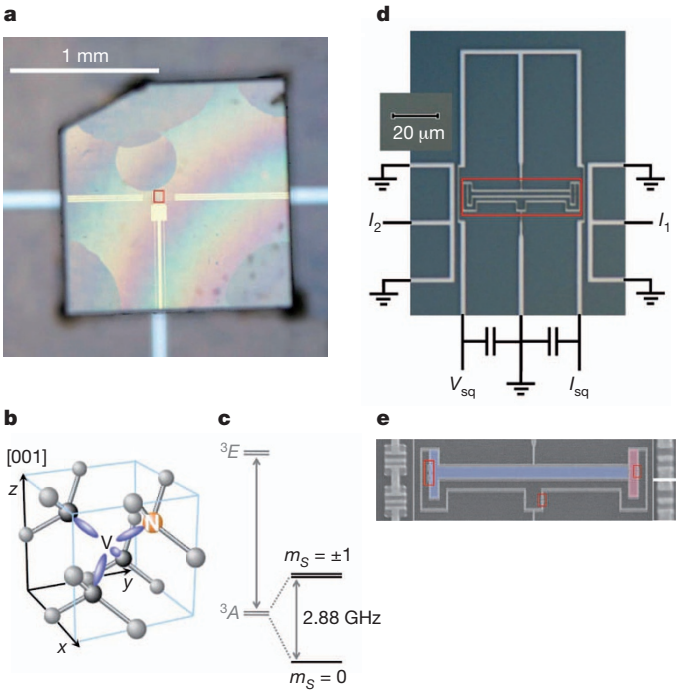

Figure 1 | Experimental set-up of a NV^- diamond sample attached to a flux qubit system. a, Diamond crystal glued on top of a flux qubit (red box). **b**, NV^- centre: V, vacancy; N, nitrogen atom. **c**, Energy diagram of the NV^- centre[28]. **d**, Optical micrograph of the superconducting circuits. The flux qubit and a superconducting quantum interference device (SQUID) detector (current, I_{sq}; voltage, V_{sq}) are highlighted (red box). Microwave control lines (I_1 and I_2) are located on both sides. **e**, Gap-tunable flux qubit and the edge-shared SQUID used as qubit state detector. The qubit contains two loops, the main loop (blue) and the α-loop (SQUID; pink), which controls the tunnelling energy of the qubit. Josephson junctions are highlighted (red boxes).

[1]NTT Basic Research Laboratories, NTT Corporation, 3-1 Morinosato-Wakamiya, Atsugi, Kanagawa 243-0198, Japan. [2]National Institute of Informatics, 2-1-2 Hitotsubashi, Chiyoda-ku, Tokyo 101-8430, Japan. [3]University of Osaka, Graduate school of Engineering Science, 1-3 Machikane-yama, Toyonaka, Osaka 560-8531, Japan. [4]PRESTO JST, 4-1-8 Honcho, Kawaguchi, Saitama 332-0012, Japan.

NV^- centres[20]. Photoluminescence optical spectroscopy (Fig. 2) established that NV^- centres were generated with a concentration of $\sim 1.1 \times 10^{18}\,cm^{-3}$ over a depth of 1 μm (see Supplementary Information, section II, for further details). We can describe the ground state of a single NV^- centre with the Hamiltonian[21]

$$H_{NV} = hDS_z^2 + hE\left(S_x^2 - S_y^2\right) + hg_e\mu_B \mathbf{B}\cdot\mathbf{S}$$

where S_x, S_y and S_z are the usual Pauli spin-one operators, the components of **S**; D is the zero-field splitting (2.878 GHz); E is the strain-induced splitting (<10 MHz); $g_e = 2$ is the nitrogen–vacancy Landé factor; $\mu_B = 14\,MHz\,mT^{-1}$ is the Bohr magneton; and h is Planck's constant. The final term represents the Zeeman splitting, which is negligible in our case because the magnetic field (**B**) applied perpendicular to the surface of the chip to prepare the flux qubit is less than 0.1 mT.

A diamond crystal was glued on top of the superconducting circuit with the ^{12}C-implanted (001) surface facing the flux qubit (Fig. 1a). The distance between the flux qubit and the surface of the diamond crystal was adjusted to be less than a micrometre. We used a gap-tunable flux qubit[22,23] (Fig. 1d, e and Supplementary Information, section I) in which the smallest of the three Josephson junctions in the qubit was replaced by a low-inductance d.c. SQUID loop (Fig. 1e, pink loop). The flux qubit/NV^- ensemble coupled system was measured by detecting the qubit state using a read-out d.c. SQUID (the biggest loop in Fig. 1e sharing edges with the flux qubit), which is inductively coupled to the qubit. When biasing the main loop at close to one-half of a flux quantum, the device is effectively a two-level system[24] described by the Hamiltonian

$$H_{qb} = \frac{h}{2}\left(\Delta\sigma_x + \varepsilon\sigma_z\right)$$

which is given in the basis of clockwise and anticlockwise qubit persistent currents. Here σ_x and σ_z are Pauli spin-half operators, $h\varepsilon = 2I_P(\Phi_{ex} - 3\Phi_0/2)$ is the energy bias ($I_P \approx 300$ nA is the persistent current in the qubit, Φ_{ex} is the external flux threading the qubit loop and $\Phi_0 = h/2e$ is the flux quantum) and Δ is the tunnel splitting. The energy splitting of the gap-tunable flux qubit is $hF = h\sqrt{\varepsilon^2 + \Delta^2}$ where ε and Δ can be controlled independently using the external magnetic flux threading the two loops. This type of flux qubit can be tuned into resonance with a NV^- ensemble *in situ* at a base temperature of ~12 mK while keeping the qubit at its optimum flux bias (degeneracy point). The total Hamiltonian of the coupled system is

$$H = \frac{h}{2}\left(\Delta\sigma_x + \varepsilon\sigma_z\right) + h\sum_i\left[DS_{z,i}^2 + E\left(S_{x,i}^2 - S_{y,i}^2\right)\right] + \frac{h}{2}\sum_i g_i\sigma_z S_{x,i}$$

where i runs over the NV^- centres that couple to the flux qubit. The corresponding coupling constant can be estimated using the Biot–Savart law as $g_i \approx 8.8$ kHz (see Supplementary Information, sections III and IV, for further details). In this set-up, states $|m_S = \pm 1\rangle_i$ of the NV^- electronic spin are nearly degenerate and our flux qubit therefore couples to both the $|0\rangle_i \rightleftharpoons |1\rangle_i$ transition and the $|0\rangle_i \rightleftharpoons |-1\rangle_i$ transition. This results in an effective coupling constant of $\sqrt{2}g_i$ when a degenerate NV^- centre is treated as a two-level system.

From the spectroscopic measurements, a clear anticrossing was observed (Fig. 3a) near the degeneracy point of the flux qubit, whereas no such gap was observed in the same flux qubit before the mounting of the ensemble (Fig. 3a, inset). We also note a narrow resonance, of width less than 1 MHz, at 2.878 GHz near this anticrossing. This can be ascribed to the near-degenerate excited states of the NV^- ensemble. From the high-resolution spectrum shown in Fig. 3b, a vacuum Rabi

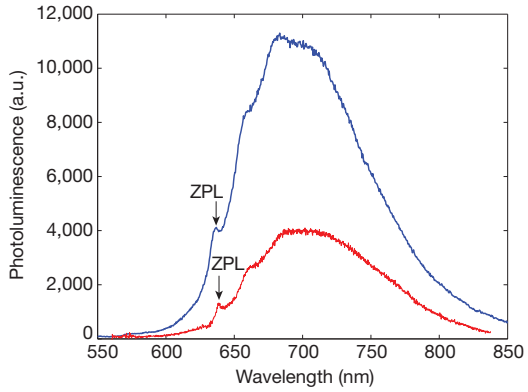

Figure 2 | Photoluminescence spectra. Spectra of ensembles of colour centres in the highly carbon-implanted sample (blue) and a single NV^- centre in pure diamond at room temperature (red). The signal intensities are normalized for comparison (a.u., arbitrary units). In the spectrum of the single NV^- centre, the contributions of phonon Raman scattering from diamond at 573 nm and between 600 and 620 nm have been subtracted[29]. The NV^- zero-phonon line (ZPL) at 637 nm is observed in both spectra[29,30]. The spectra are similar to each other and those reported previously[29,30], indicating that NV^- centres are abundant in the implanted sample. The signal intensity of the ensemble is $\sim 6.5 \times 10^4$ that of the single centre, and we estimate the concentration of NV^- centres to be $1.1 \times 10^{18}\,cm^{-3}$.

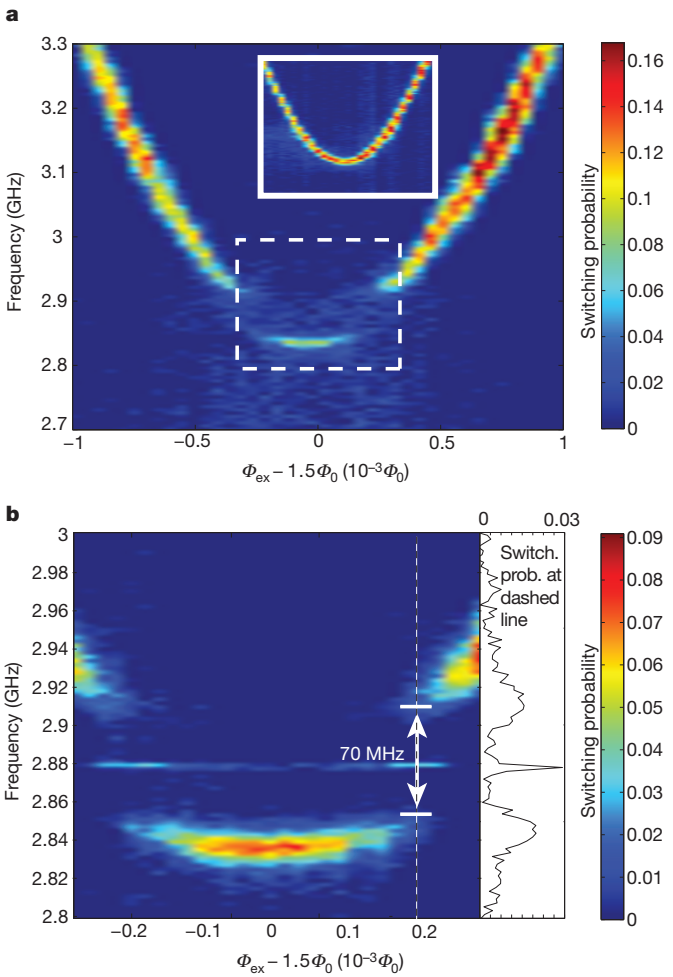

Figure 3 | Energy spectrum of the flux qubit coupled to a NV^- ensemble. **a**, Resonant frequencies indicated by the SQUID detector switching probability (when a 500-ns microwave pulse excites the system before the read-out pulse) versus the external magnetic flux, $\Phi_{ex} = \Phi_m + \Phi_\alpha/2$, where Φ_m and Φ_α are the fluxes through the qubit main loop and the qubit α-loop, respectively. Inset, spectrum over the same region before mounting of the diamond crystal. **b**, Magnified view of the dashed region in **a**, including a cross-sectional view of the cut along the dashed line. A vacuum Rabi splitting of 70 MHz is observed. Because the qubit phase relaxation time is $T_2^{echo} \approx 0.25\,\mu s$, we are operating in the strong-coupling regime.

splitting near $g_{ens} \approx 70$ MHz was clearly observed, confirming strong coupling (two broad resonance peaks are present in the cross-sectional view) between the flux qubit and the NV^- ensemble. The ensemble can be seen as an effective harmonic oscillator strongly coupled to the flux qubit[17]. Next, from the measured vacuum Rabi splitting and our calculated value of g_i, we can estimate the number of NV^- centres in the coupled ensemble to be $N = g_{ens}^2/2g^2 \approx 3.2 \times 10^7$, where the factor of two in the denominator is due to the twofold degeneracy of the excited states $|\pm 1\rangle_i$ of a NV^- centre. This estimate is consistent with the density of NV^- centres measured by photoluminescence spectroscopy of the whole sample (1.1×10^{18} cm^{-3}) multiplied by the volume of centres coupling to the flux qubit (40 μm^2 (area) × 0.7 μm (effective thickness)). This spectroscopy approach gives the number of coupled centres as $\sim 3.1 \times 10^7$.

Next we investigated the dynamics of our system in the time domain, with a measurement cycle similar to that used in systems of qubits coupled with LC (inductor–capacitor) resonators[25] (Fig. 4a, inset). We first excited the flux qubit and then brought it into resonance with the NV^- ensemble. Single-energy quantum exchange between the flux qubit and the NV^- ensemble at resonance manifests itself as the vacuum Rabi oscillations

$$|1\rangle_{qb}|0\rangle_{ens} \rightleftharpoons |0\rangle_{qb}|1\rangle_{ens}$$

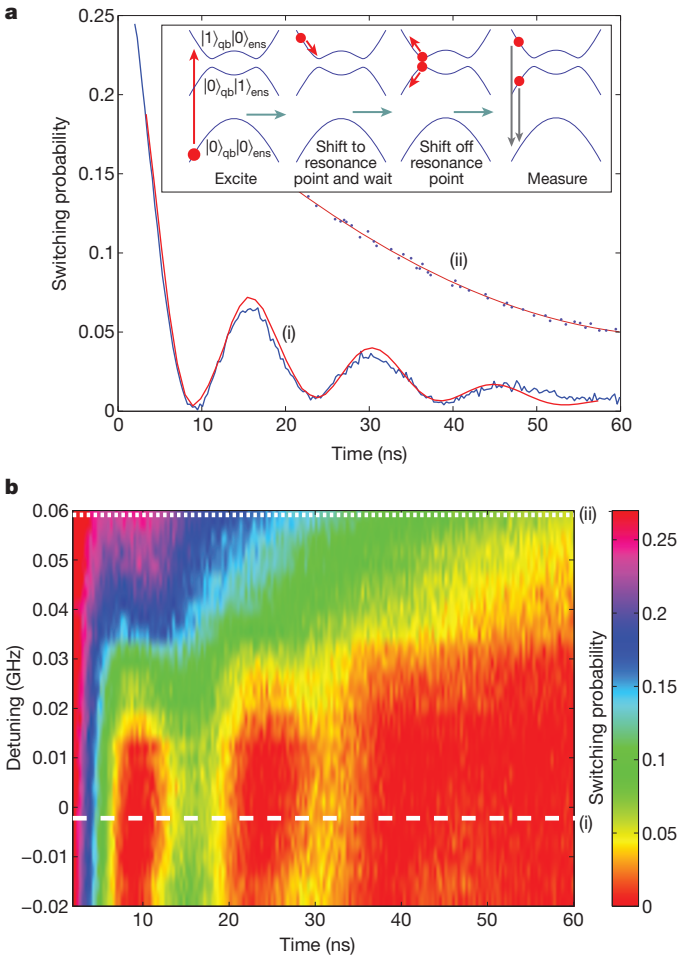

Figure 4 | Vacuum Rabi oscillations of the flux qubit/NV^- ensemble coupled system. a, Line (i): damped oscillation (blue) of an initially excited flux qubit resonantly coupled to a NV^- ensemble. The red line shows the results of a numerical model (Supplementary Information, section III). Line (ii): the same sequence as in line (i), but with 60-MHz detuning from resonance. Inset, measurement sequence. **b**, Two-dimensional plot of the SQUID detector switching probability as a function of both time and the detuning by flux bias shift. The white dashed and dotted lines correspond to the switching probabilities shown in **a** (as indicated).

where $|0\rangle_{qb}$ and $|1\rangle_{qb}$ are respectively the ground and excited states of the qubit; $|0\rangle_{ens} = |00\cdots0\rangle$ is the ground state of the ensemble, with each individual NV^- centre in the state $|m_S = 0\rangle$; and $|1\rangle_{ens}$ is a Dicke state of the spin ensemble with one excitation, written as $|1\rangle_{ens} = (1/\sqrt{N})\sum_i S_{+,i}|00\cdots0\rangle$. Here the operator $S_{+,i} = (1/\sqrt{2})\left[|1\rangle_i\langle 0|_i + |-1\rangle_i\langle 0|_i\right]$ excites the ith NV^- spin into a superposition of states $|1\rangle$ and $|-1\rangle$.

Figure 4a shows vacuum Rabi oscillations between the flux qubit and the ensemble of electronic spins at the 2.878-GHz resonance. However, the decay time of the oscillations is approximately 20 ns. This is much shorter than the relaxation times of both the flux qubit ($T_{1,qb} \approx 150$ ns) and the NV^- ensemble ($T_{1,NV} \gg 10$ μs). We cannot improve the vacuum Rabi decay time even by tuning the qubit degeneracy point closer to the NV^- resonance frequency. As we tune the flux qubit away from the 2.878-GHz resonance, by changing Φ_m (Supplementary Information, section I), the coherence time associated with this measurement scheme becomes considerably longer (Fig. 4a, line (ii), and Fig. 4b). From these results, we conclude that a strong source of dephasing of unknown origin exists in the system near resonance.

There are several likely sources of dephasing. The most probable is a large electron spin-half bath derived from the P1 centres (a nitrogen atom substituting a carbon atom) present in the HPHT-synthesized type-Ib diamond crystal used to prepare the NV^- ensemble. In our situation, where there is no external magnetic field, the NV^- centres and P1 centres naturally couple[12], in which case an enhanced decay may result[26]. The effect of P1 centres can be eliminated to a large extent by applying an external magnetic field to split the NV^- states $|\pm 1\rangle$. A 1-mT field could split these by approximately 15 MHz, detuning them relative to the P1 centres and thus considerably improving the dephasing time of the coupled system. We can also decrease the number of P1 centres in the sample (from 100 p.p.m. to 1 p.p.m.) by using differently synthesized diamond crystals. In addition, by using non-HPHT-synthesized type-Ib crystals we can remove the effect of other natural defects that may be present. Finally, there is also a strong hyperfine interaction (~ 100 MHz) between the NV^- electron spin and ^{13}C nuclear spins. If the nuclear spins are not initially polarized, unwanted dephasing will result. Polarizing the nuclear spins, thus removing this source of dephasing, should allow us to observe vacuum Rabi oscillations where we are limited by the dephasing time of the flux qubit.

In conclusion, we have experimentally demonstrated strong coherent coupling between a flux qubit and an ensemble of nitrogen–vacancy colour centres in single-crystal diamond. Furthermore, we have observed, via vacuum Rabi oscillations, the coherent exchange (transfer) of a single quantum of energy. This is the first step towards the realization of a long-lived quantum memory for condensed-matter systems, with an additional potential future application as an interface between the microwave and optical domains.

METHODS SUMMARY

Photoluminescence of the NV^- centres. A confocal microscope was used to measure the photoluminescence of NV^- centres with excitation from a Nd:YAG laser[27] (wavelength, 532 nm). The photon antibunching was measured using a Hanbury Brown/Twiss set-up to identify the single NV^- centre. In the confocal microscopy, the signal intensity depends on the number of colour centres in the detected spot region, which is limited by the wavelength of the incident light and the numerical aperture of the objective lens. From the ratio, P, of the respective photoluminescence intensities of the single NV^- centre and the ensemble, the concentration of the ensemble of the NV^- centres, C, can be estimated from $C = P/V$, where V is the volume of the detected region (5.85×10^7 nm^3). We measured the ratio to be $P = (6.45 \pm 0.30) \times 10^4$, and so estimated C to be 1.1×10^{18} cm^{-3}.

Spectroscopy of the flux qubit. To make spectroscopic measurements, we used a 500-ns-long microwave pulse to excite the flux qubit. This was followed by a readout pulse on the d.c. SQUID that determines the detector's switching probability and allows us to infer the state of the flux qubit.

Received 30 May; accepted 10 August 2011.

1. Clarke, J. & Wilhelm, F. K. Superconducting quantum bits. *Nature* **453,** 1031–1042 (2008).
2. Nakamura, Y., Pashkin, YuA & Tsai, J. S. Coherent control of macroscopic quantum states in a single-Cooper-pair box. *Nature* **398,** 786–788 (1999).
3. Vion, D. *et al.* Manipulating the quantum state of an electrical circuit. *Science* **296,** 886–889 (2002).
4. Chiorescu, I., Nakamura, Y., Harmans, C. J. P. M. & Mooij, J. E. Coherent quantum dynamics of a superconducting flux qubit. *Science* **299,** 1869–1871 (2003).
5. Sillanpää, M. A., Park, J. I. & Simmonds, R. W. Coherent quantum state storage and transfer between two phase qubits via a resonant cavity. *Nature* **449,** 438–442 (2007).
6. Majer, J. *et al.* Coupling superconducting qubits via a cavity bus. *Nature* **449,** 443–447 (2007).
7. DiCarlo, L. *et al.* Demonstration of two-qubit algorithms with a superconducting quantum processor. *Nature* **460,** 240–244 (2009).
8. Ansmann, M. *et al.* Violation of Bell's inequality in Josephson phase qubits. *Nature* **461,** 504–506 (2009).
9. Sørensen, A. S. van der Wal, C. H., Childress, L. I. & Lukin, M. D. Capacitive coupling of atomic systems to mesoscopic conductors. *Phys. Rev. Lett.* **92,** 063601 (2004).
10. Tian, L., Rabl, P., Blatt, R. & Zoller, P. Interfacing quantum-optical and solid-state qubits. *Phys. Rev. Lett.* **92,** 247902 (2004).
11. Rabl, P. *et al.* Hybrid quantum processors: molecular ensembles as quantum memory for solid state circuits. *Phys. Rev. Lett.* **97,** 033003 (2006).
12. Marcos, D. *et al.* Coupling nitrogen-vacancy centers in diamond to superconducting flux qubits. *Phys. Rev. Lett.* **105,** 210501 (2010).
13. Brune, M. *et al.* Quantum Rabi oscillation: a direct test of field quantization in a cavity. *Phys. Rev. Lett.* **76,** 1800–1803 (1996).
14. Chiorescu, I., Groll, N., Bertaina, S., Mori, T. & Miyashita, S. Magnetic strong coupling in a spin-photon system and transition to classical regime. *Phys. Rev. B* **82,** 024413 (2010).
15. Wu, H. *et al.* Storage of multiple coherent microwave excitations in an electron spin ensemble. *Phys. Rev. Lett.* **105,** 140503 (2010).
16. Schuster, D. I. *et al.* High-cooperativity coupling of electron-spin ensembles to superconducting cavities. *Phys. Rev. Lett.* **105,** 140501 (2010).
17. Kubo, Y. *et al.* Strong coupling of a spin ensemble to a superconducting resonator. *Phys. Rev. Lett.* **105,** 140502 (2010).
18. Amsüss, R. *et al.* Cavity QED with magnetically coupled collective spin states. *Phys. Rev. Lett.* **107,** 060502 (2011).
19. Raizen, M. G., Thompson, R. J., Brecha, R. J., Kimble, H. J. & Carmichael, H. J. Normal-mode splitting and linewidth averaging for two-state atom in an optical cavity. *Phys. Rev. Lett.* **63,** 240–243 (1989).
20. Naydenov, B. *et al.* Enhanced generation of single optically active spins in diamond by ion implantation. *Appl. Phys. Lett.* **96,** 163108 (2010).
21. Neumann, P. *et al.* Excited-state spectroscopy of single NV defects in diamond using optically detected magnetic resonance. *N. J. Phys.* **11,** 013017 (2009).
22. Zhu, X., Kemp, A., Saito, S. & Semba, K. Coherent operation of a gap-tunable flux qubit. *Appl. Phys. Lett.* **97,** 102503 (2010).
23. Fedorov, A. *et al.* Strong coupling of a quantum oscillator to a flux qubit at its symmetry point. *Phys. Rev. Lett.* **105,** 060503 (2010).
24. Mooij, J. E. *et al.* Josephson persistent-current qubit. *Science* **285,** 1036–1039 (1999).
25. Johansson, J. *et al.* Vacuum Rabi oscillations in a macroscopic superconducting qubit LC oscillator system. *Phys. Rev. Lett.* **96,** 127006 (2006).
26. Hanson, R., Dobrovitski, V. V., Feiguin, A. E., Gywat, O. & Awschalom, D. D. Coherent dynamics of a single spin interacting with an adjustable spin bath. *Science* **320,** 352–355 (2008).
27. Mizuochi, N. *et al.* Coherence of single spins coupled to a nuclear spin bath of varying density. *Phys. Rev. B* **80,** 041201(R) (2009).
28. Jelezko, F., Gaebel, T., Popa, I., Gruber, A. & Wrachtrup, J. Observation of coherent oscillations in a single electron spin. *Phys. Rev. Lett.* **92,** 076401 (2004).
29. Gruber, A. *et al.* Scanning confocal optical microscopy magnetic resonance on single defect centers. *Science* **276,** 2012–2014 (1997).
30. Kurtsiefer, Ch, Zarda, P., Mayer, S. & Weinfurter, H. A stable solid-state source of single photons. *Phys. Rev. Lett.* **85,** 290–293 (2000).

Supplementary Information is linked to the online version of the paper at www.nature.com/nature.

Acknowledgements We thank T. Tawara, H. Gotoh and T. Sogawa for optical measurements at an early stage of this work. We also thank H. Tanji, Y. Matsuzaki, S. J. Devitt, J. Schmiedmayer and J. E. Mooij for discussions. This work was supported in part by the Funding Program for World-Leading Innovative R&D on Science and Technology (FIRST), Scientific Research of Specially Promoted Research (grant no. 18001002) by MEXT, a Grant-in-Aid for Scientific Research on Innovative Areas (grant no.22102502), and Scientific Research (A) grant no. 22241025 from the Japanese Society for the Promotion of Science (JSPS). M.S.E. was supported by a JSPS fellowship.

Author Contributions All authors contributed extensively to the work presented in this paper. X.Z. and A.K. carried out measurements and data analysis on the coupled flux qubit/NV^{-} ensemble. N.M., M.K. and K.S. prepared and characterized the NV^{-} diamond crystals. X.Z., S.K., S.S. and A.K. designed and fabricated the flux qubit and associated devices. S.S., K.K. and A.K. designed and developed the flux qubit measurement system. W.J.M., A.K., Y.T., H.N., M.S.E. and K.N. provided theoretical support and analysis. X.Z., M.S.E., W.J.M. and K.S. wrote the manuscript, with feedback from all authors. W.J.M. and K.S. designed and supervised the project.

Author Information Reprints and permissions information is available at www.nature.com/reprints. The authors declare no competing financial interests. Readers are welcome to comment on the online version of this article at www.nature.com/nature. Correspondence and requests for materials should be addressed to K.S. (semba.kouichi@lab.ntt.co.jp).